Alexandria Engineering Journal 78 (2023) 426–437

Contents lists available at ScienceDirect

Alexandria Engineering Journal

journal homepage: www.elsevier.com/locate/aej

Original Article

Three-dimensional transient CFD modeling of multiple finned aluminum foam heat sinks in a horizontal channel

Boulahrouz Salim [a,b,*], Saoudi Abdenour [b,c], Chahaoui Oualid [b,c], Hadi M. Marwani [d], Rokkaya Sami [e], N.I. Aljuraide [f], Raed H. Althomali [g], Mohammed M. Rahman [d,h,*], Meser M. Ali [i], M.A. El Bouz [j]

[a] Electromechanical Engineering Laboratory, Badji Mokhtar – Annaba University, 23000, Algeria
[b] Department of Mechanical Engineering, Abbes Laghrour University, Khenchela 40004, Algeria
[c] Laboratory of Engineering and Sciences of Advanced Materials (ISMA), Abbes Laghrour University Khenchela, 40004, Algeria
[d] Chemistry Department, Faculty of Science, King Abdulaziz University, Jeddah 21589, Saudi Arabia
[e] Department of Science, College of Sciences, Taif University, P.O. 11099, Taif 21944, Saudi Arabia
[f] Department of Physics, Turabah Branch, Turabah University College, Taif University, P.O. Box 11099, Taif 21944, Saudi Arabia
[g] Department of Chemistry, College of Art and Science, Prince Sattam bin Abdulaziz University, Wadi Al-Dawasir 11991, Saudi Arabia
[h] Center of Excellence for Advanced Materials Research (CEAMR), King Abdulaziz University, Jeddah 21589, Saudi Arabia
[i] Cellular and Molecular Imaging Laboratory, Department of Neurosurgery, Henry Ford Hospital, Box 82, Detroit, MI, USA
[j] Mechanical Power Engineering Department, Faculty of Engineering, Mansoura University, P.O. Box 35516 Mansoura, Egypt

ARTICLE INFO

Keywords:
Finned aluminum foam heat sinks
Cooling electronics
Numerical simulation
Forchheimer-Brinkman extended Darcy model
Forced convection

ABSTRACT

Finned metal foam heat sinks are well-known because of their excellent performance in cooling of powered electronics. In this study, three-dimensional transient numerical simulations of finned aluminum foam heat sinks in a forced convection of air were carried out using commercial COMSOL. The geometry under consideration consists of an array of finned aluminum foam heat sinks mounted on heater blocks and placed on a plate in a horizontal channel. Heat sink aluminum foam regions were considered as porous media with a local non-equilibrium thermal model to evaluate thermal characteristics, while the Forchheimer-Brinkman extended Darcy model is considered for the flow analysis. Our main concern in the present study is to evaluate the transient thermal–hydraulic behavior and the cooling performance under constant flux heat sources while varying the Reynolds number and variable morphological parameters of the aluminum foam, i.e., porosity (ε) varied from 0.85 to 0.95. The thermal performance ratio and the average Nusselt number of the finned aluminum foam heat sinks are 23.14% and 30%, respectively, larger than the finned aluminum heat sinks. As the Reynolds number increases, the thermal characteristics are enhanced, and the pressure drop is increased. An increase in porosity causes a reduction in heat transfer rate and an elevation of pressure drop.

1. Introduction

Advanced technology is increasingly being used for compact electronic components and very high computing power, producing excessive heat in circuits. In the near future, the specific heat flux generated by the high-power electronic devices will exceed 1000 W/cm^2, and to ensure high efficiency and optimal lifetime of these devices, an efficient and fast cooling process is required. Conventional heat sinks have reached their limits in attempting to guarantee the cooling processes for this advanced electronic technology [1–6]. Metallic foam has a light weight and a high surface/volume ratio (1000–3000 m^2/m^3), which provides an excellent opportunity to enhance heat exchange with a forced fluid during cooling. It should also be noted that several recent solar collector applications use metallic foams at the exchange surfaces to enhance thermal performance [7–11]. Currently metallic foams are used in composite structures with phase change materials in the field of latent heat storage to improve quality and performance [12], as well as used to enhance heat exchange in different types of heat exchangers [13].

Experiments were performed by Dukhan et al [14] on the cooling

* Corresponding authors.
E-mail addresses: boulahrouz.salim@univ-khenchela.dz (B. Salim), saoudi_abdenour@univ-khenchela.dz (S. Abdenour), oualid.chahaoui@univ-khenchela.dz (C. Oualid), hmarwani@kau.edu.sa (H.M. Marwani), rokayya.d@tu.edu.sa (R. Sami), n.aljareed@tu.edu.sa (N.I. Aljuraide), r.althomali@psau.edu.sa (R.H. Althomali), mmrahman@kau.edu.sa (M.M. Rahman), mali8@hfhs.org (M.M. Ali), mostafa_booz@yahoo.com (M.A. El Bouz).

https://doi.org/10.1016/j.aej.2023.07.074
Received 30 January 2023; Received in revised form 13 July 2023; Accepted 28 July 2023

Nomenclature

c_p	heat capacity of fluid (J kg^{-1} K^{-1})
D_h	hydraulic diameter (m)
f	friction factor (–)
h	convective heat coefficient (W m^{-2} K^{-1})
k	thermal conductivity of fluid (W m^{-1} K^{-1})
Nu	Nusselt number (–)
P_f	thermal performance ratio (–)
p	pressure (Pa)
Δp	pressure drop (Pa)
Re	Reynolds number (–)
q_w	thermal source heat flux (W)
T	temperature (K)
t	time (s)
V	air velocity (m/s)
U_{in}	air velocity entering channel (m/s)

Greek symbols

α	thermal diffusivity (m^2 s^{-1})
ρ	fluid density (kg m^{-3})
μ	fluid viscosity (kg m^{-1} s^{-1})

Subscripts

f	fluid
s	solid
m	average
w	wall
in	input

Abbreviations

FAFHS	Finned aluminum foam heat sink
FAHS	Finned aluminum heat sink
AF	Aluminum foam
AFHS	Aluminum foam heat sink

process with water as a coolant in two porous media: metal foam and packed spheres. The authors proposed an equation to evaluate the pressure drop in porous media. Suleiman et al. [15] numerically investigated the metallic foam with open cells; they determined the thermal characteristics and compared them to those found analytically, which showed good agreement. Experimental studies were conducted by Dukhan et al [16] on a cylinder made of metal foam, cooled by water and exposed to an imposed thermal flux. They discussed the different flow regimes established inside the cylinder: Darcy, transitional, and Forchheimer. They proposed an analytical solution for the thermal analysis whose results coincide perfectly with their experimental results. Combined experimental and numerical investigations were performed by Bayomy et al. [17] to analyze the cooling process of a developed processor using a water-cooled metal foam block. The authors have shown that water as a cooler shows better thermal performance than air. Paknezhada et al. [18] investigated the temperature distribution of a flat plate exposed to an imposed heat flux with and without heat sink made of metallic foam in a free-convection environment. They found that the overall cooling efficiency using foam at a 90° inclination angle is approximately 17%.

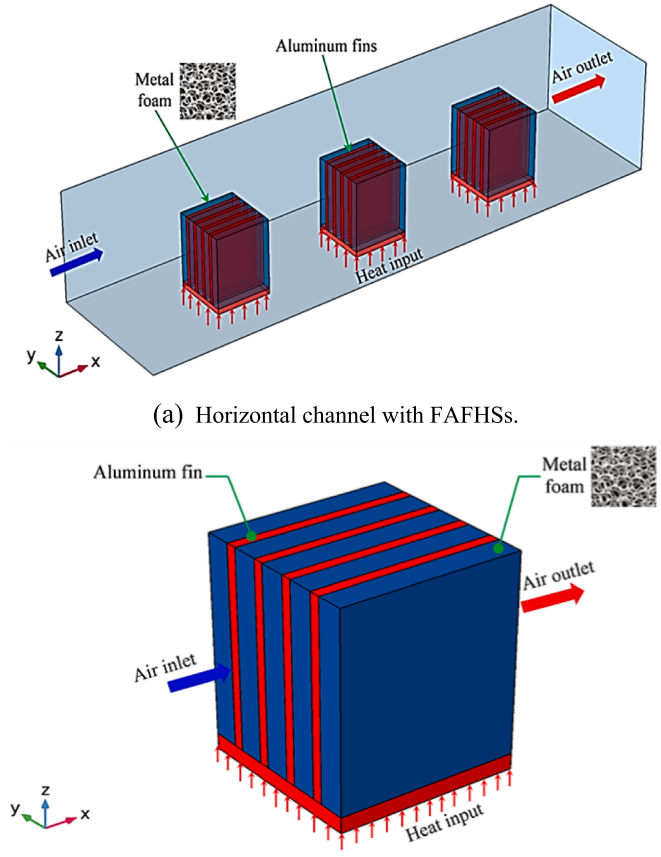

Fig. 1. Principal diagram of (a) horizontal channel with FAFHSs, and (b) FAFHS.

Mohammadian and Zhang [19] undertook numerical study to investigate the thermal management of a lithium-ion battery using porous matrices with air-cooled pin fins. They showed that a porous aluminum matrix with aluminum fins subjected to air-cooled flow is an excellent alternative for improving the cooling capacity inside the battery cell. Li et al. [20] analyzed two types of heat sinks: the first type included metal foam only, and the second type incorporated pin fins within the porous matrix. They showed that the second configuration provides a high thermal performance, low thermal resistance, and a suitable pressure drop.

A detailed review of the literature reveals that despite the numerous theoretical and experimental studies conducted on metallic foams, very few studies have analyzed the three-dimensional transient behavior of multiple finned aluminum foam heat sinks (FAFHSs) in a channel. Moreover, the impacts of the foam porosity on the thermal–hydraulic behavior and cooling performance have rarely been reported. The purpose of the present study is to evaluate the cooling performance and the thermal–hydraulic behavior of an array of air-cooled finned aluminum foam heat sinks mounted on thermal sources inside a horizontal channel. To achieve this objective, transient three-dimensional numerical simulations have been performed using the commercial software COMSOL. The study focuses on the impacts of foam porosity parameter at varying Reynolds number on the thermal–hydraulic characteristics of the heat sinks. The novelty of this study lies in the numerical evaluation of the transient thermal–hydraulic behavior and cooling performance of multiple air-cooled finned aluminum foam heat sinks used to cool power electronic devices. Heat dissipation occurs under forced convection and constant heat flow, while varying the inlet air velocity and the porosity of the aluminum foam.

2. Problem description and assumptions

We consider a laminar flow of air inside a horizontal channel of rectangular cross-section, in which three FAFHSs are placed on its

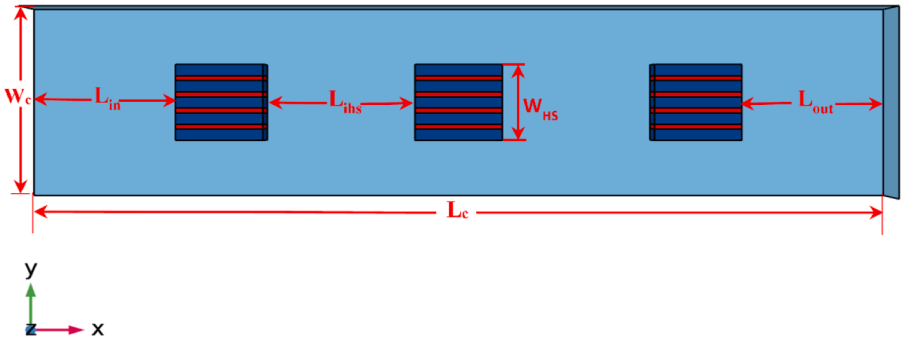

(a) Channel with FAFHSs.

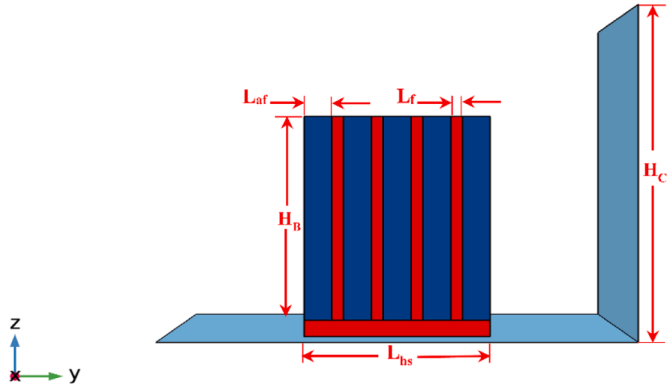

(b) FAFHS.

Fig. 2. Geometrical dimensions of (a) channel with FAFHSs, and (b) FAFHS.

bottom side (Fig. 1). Each FAFHS consists of a square base of aluminum to which five rectangular aluminum foam fins (AFFs) and four aluminum fins (AFs) are attached. The detailed geometrical dimensions of the channel and FAFHSs are listed in Fig. 2 and Table 1. Air with constant thermo-physical properties was utilized as a coolant fluid. As cited below in the section on boundary conditions related to the physical model, all sides of the channel except the base are considered adiabatic. At the channel inlet, a constant velocity of air was considered, and at the channel outlet, a zero pressure (p = 0 Pa) was specified. To simulate the cooling conditions of an electronic device, a constant heat flux (q_w = 4 W) was generated using a thermal source at the base of each FAFHS.

The assumptions of the physical model are as follows:

- Aluminum foam is an isotropic and uniform porous material.
- The air used as a coolant is considered as viscous, Newtonian, and incompressible.
- The air flow is considered as laminar.
- In the energy equation, the viscous dissipation term is negligible.
- Thermal contact resistances are neglected.

3. Mathematical formulation and boundary and initial conditions

The conservation equations related to the physical model describe the thermal and fluid flow behavior in three distinct regions: (1) the pure fluid region is modeled by the Navier–Stokes equations; (2) the metal foam region, where the Forchheimer-Brinkman extended Darcy model equations and the local thermal non-equilibrium model are used; (3) the aluminum fins regions are modeled by the heat equation.

(1) Pure fluid region

The conservation equations in fluid region in the channel are given as [21]:

- Continuity equation:

$$\nabla\left(\vec{V}\right) = 0 \tag{1}$$

- Momentum conservation equations:

$$\frac{\partial \vec{V}}{\partial t} + \left(\vec{V} \bullet \nabla\right)\vec{V} = -\frac{1}{\rho_f}\nabla p + \frac{\mu}{\rho_f}\nabla^2\vec{V} \tag{2}$$

- Energy conservation equation:

$$\frac{\partial T_f}{\partial t} + \vec{V} \bullet \nabla T_f = \alpha_f \nabla^2 T_f \tag{3}$$

Table 1
Detailed geometrical dimensions.

Dimensions	Values (mm)
Length of the channel L_c	400
Width of the channel W_c	100
Height of the channel H_c	80
X-axis position of the first FAFHS L_{in}	70
Y-axis position of the first FAFHS W_{HS}	30
X-axis distance to the channel exit of the last FAFHS L_{out}	70
FAFHSs spacing L_{ihs}	70
Length of the FAFHS's base L_{HS}	40
Height of the FAFHS's base H_{HS}	4
Length of the AFF L_{af}	6
Height of the AFF H_B	50
Length of the AF L_f	6

Table 2
Numerical results and comparison of the grid independence study.

Mesh type	No. of elements	Maximum element size	Minimum element size	Maximum growth rate	Curvature resolution	p (Pa)	Δp (%)	V (m/s)	ΔV (%)	T (K)	ΔT (%)
Finer	1,914,469	0.825	0.06	1.4	0.4	101327.7471	–	0.7381	–	298.8199	–
Fine	688,071	1.2	0.15	1.45	0.5	101327.7494	2e-6	0.7400	0.25	299.1278	0.1
Normal	263,958	1.5	0.27	1.5	0.6	101327.6681	7e-5	0.7182	0.25	299.1277	0.1

Table 3
Properties of aluminum-alloy T-6201 foam with various porosities [30].

ε	d_f (mm)	d_p (mm)	K (m^2)	C_F	α_{sf} (m^{-1})
0.85	0.4	2.62	6.20×10^{-8}	0.058	1536
0.90	0.4	3.02	1.05×10^{-7}	0.078	1089
0.925	0.4	3.22	1.37×10^{-7}	0.089	886
0.95	0.4	3.32	1.65×10^{-7}	0.099	701

(2) Aluminum foam region (porous media).

- Mass conservation equation:

$$\nabla\left(\vec{V}\right) = 0 \tag{4}$$

- Momentum conservation equations:

$$\frac{1}{\varepsilon}\frac{\partial \vec{V}}{\partial t} + \frac{1}{\varepsilon}\left(\vec{V} \bullet \nabla\right)\vec{V} = -\frac{1}{\rho_f}\nabla p + \frac{\mu}{\varepsilon}\nabla^2\vec{V} - \frac{\mu}{K}\vec{V} - \frac{\varepsilon C_F}{K^{1/2}}\left|\vec{V}\right|\vec{V} \tag{5}$$

- Energy conservation equation (fluid phase):

$$\varepsilon\left(\rho c_p\right)_f\frac{\partial T_f}{\partial t} + \left(\rho c_p\right)_f\vec{V} \bullet \nabla T_f = \varepsilon\nabla \bullet \left(\left(k_f + k_s\right)\nabla T_f\right) + h_{sf}\alpha_{sf}\left(T_s - T_f\right) \tag{6}$$

- Energy conservation equation (solid phase):

$$(1-\varepsilon)\left(\rho c_p\right)_s\frac{\partial T_s}{\partial t} = (1-\varepsilon)\nabla \bullet \left(k_s\nabla T_s\right) + h_{sf}\alpha_{sf}\left(T_f - T_s\right) \tag{7}$$

Table 3 provides the value of α_{sf}, which represents the density of the contact surface between the two solid and fluid phases; h_{sf} which the heat transfer coefficient between the solid and fluid phases is given by the following correlation [22]:

$$h_{sf} = \left(0.52Re_{d_f}^{0.5}Pr^{O.37}\right)\left(\frac{k_f}{d_f}\right) \tag{8}$$

where the Reynolds number referenced to the fiber diameter can be expressed as follows:

$$Re_{d_f} = \frac{\rho_f u d_f}{\mu_f} \tag{9}$$

(3) Aluminum fin region

$$\left(\rho c_p\right)_s\frac{\partial T_s}{\partial t} = \nabla \bullet \left(k_s\nabla T_s\right) \tag{10}$$

The hydraulic diameter is defined as:

$$D_h = \frac{4(H_c \bullet W_c)}{2(H_c + W_c)} \tag{11}$$

where H_c and W_c are the height and the width of the channel, respectively; U_{in} is the air velocity at the inlet of the channel; p_0 is the atmospheric pressure; θ is the dimensionless temperature; and q_w is the flux-heat source. The permeability K and the coefficient of inertia C_F are given by Table 3 [23] cited below.

The dimensionless temperature is defined as [24]:

$$\theta = \frac{T - T_{am}}{q_w H_B / k_{s,eff}} \tag{12}$$

where H_B is the height of the AFF; $k_{s,eff}$ is the effective thermal conductivity of the aluminum foam cited in the reference [24]; and T_{am} is

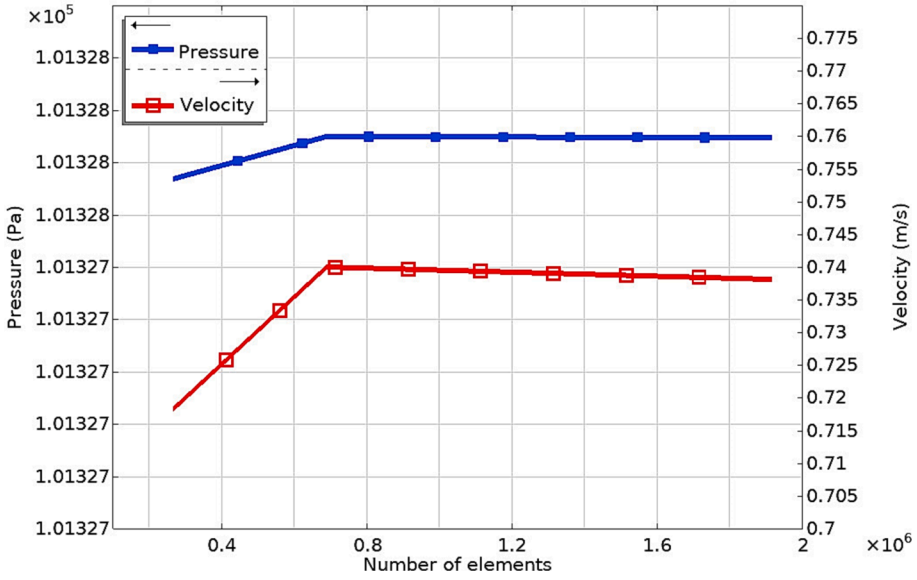

Fig. 3. Grid independence test.

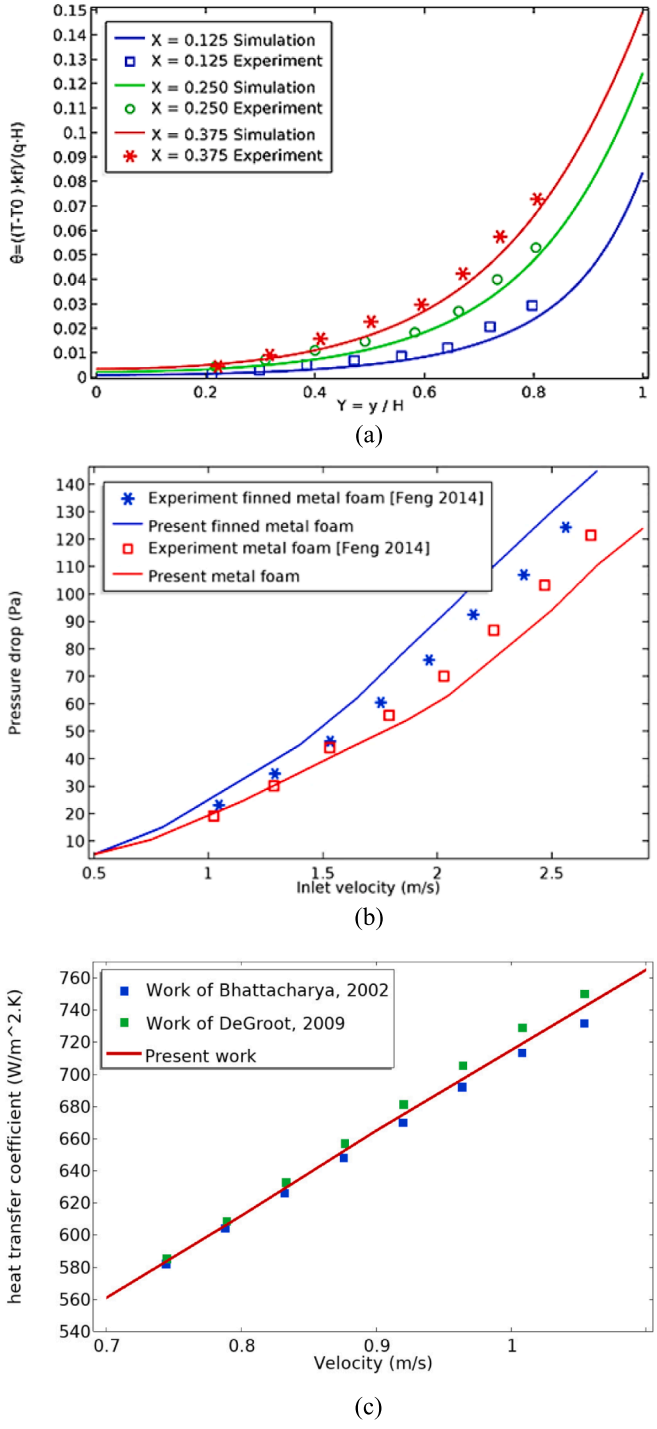

Fig. 4. Validation with experimental data cited in Refs. [23,24,28] and [29] for AF and FAFHS: (a) temperature, (b) pressure drop; and (c) heat transfer coefficient.

the ambient temperature.

The coefficient f is the friction factor expressed as follows [25]:

$$f = \frac{(\Delta p/L)H_B}{\frac{1}{2}\bullet\left(\rho_f U_{in}^2\right)} \tag{13}$$

The corresponding Reynolds number is [25]:

$$Re = \frac{\rho_f u D_h}{\mu_f} \tag{14}$$

The average Nusselt number is given as [25]:

$$Nu_m = \frac{h_m H_B}{k_f} = \frac{q_w H_B}{\left(T_{w,m} - T_{f,m}\right)} \tag{15}$$

The thermal performance ratio (P_f) defines the increase in the average Nusselt number and the resulting flow resistance between the finned aluminum foam heat sink (FAFHS) and the finned aluminum heat sink (FAHS), as shown below [25]:

$$P_f = \frac{Nu_{m,FAF}/Nu_{m,FA}}{\left(f_{FAF}/f_{FA}\right)^{1/3}} \tag{16}$$

As described in the boundary conditions section cited below, all walls of the channel except the bottom wall are considered as adiabatic. The internal walls and FAFHSs bases are described using no-slip boundary conditions, and a constant heat flux is generated by the thermal sources. The initial and boundary conditions that are utilized in this study are as follows:

(1) At the channel inlet ($x = 0$, $0 \le y \le W_C$, and $0 \le z \le H_C$).

$$u = U_{in},\ v = w = 0,\ T = T_{am}$$

where T_{am} is the ambient temperature; p_0 is the atmospheric pressure.

(2) At the bottom side of the channel ($z = 0$, $0 \le x \le L_C$, $0 \le y \le W_C$), no-slip conditions are employed.

$$u = v = w = 0$$

Without heater:

$$\frac{\partial T_f}{\partial z} = 0,\ \frac{\partial T_s}{\partial z} = 0$$

With heater:

$$q_w = -k_f\frac{\partial T_f}{\partial z} - k_s\frac{\partial T_s}{\partial z}$$

(3) At the top of the channel ($z = H_C$, $0 \le x \le L_C$, $0 \le y \le W_C$), no-slip and insulated wall conditions are employed.

$$u = v = w = 0$$

$$\frac{\partial T_f}{\partial z} = 0,\ \frac{\partial T_s}{\partial z} = 0$$

(4) Along the two sidewalls ($y = 0$ and $y = W_C$, $0 \le x \le L_C$, $0 \le z \le H_C$), no-slip and insulated wall conditions are employed.

$$u = v = w = 0$$

$$\frac{\partial T_f}{\partial y} = \frac{\partial T_s}{\partial y} = 0$$

(5) At the channel exit ($x = L_C$, $0 \le y \le W_C$, $0 \le z \le H_C$), the fully development conditions are verified.

$$\frac{\partial u}{\partial x} = \frac{\partial v}{\partial x} = \frac{\partial w}{\partial x} = 0$$

$$\frac{\partial T_f}{\partial x} = 0,\ p = 0$$

(6) Aluminum fins and aluminum foam fins interfaces:

$$\left[-k_s\frac{\partial T_s}{\partial n}\right]_A = \left[-k_f\frac{\partial T_f}{\partial n} - k_s\frac{\partial T_s}{\partial n}\right]_{AF},\ [T_s]_A = [T_f]_{AF} = [T_s]_{AF},$$

$$u = v = w = 0$$

(7) Initial conditions:

$$t = 0,\ u = U_{in},\ v = w = 0,\ T = T_{am},\ p = p_0$$

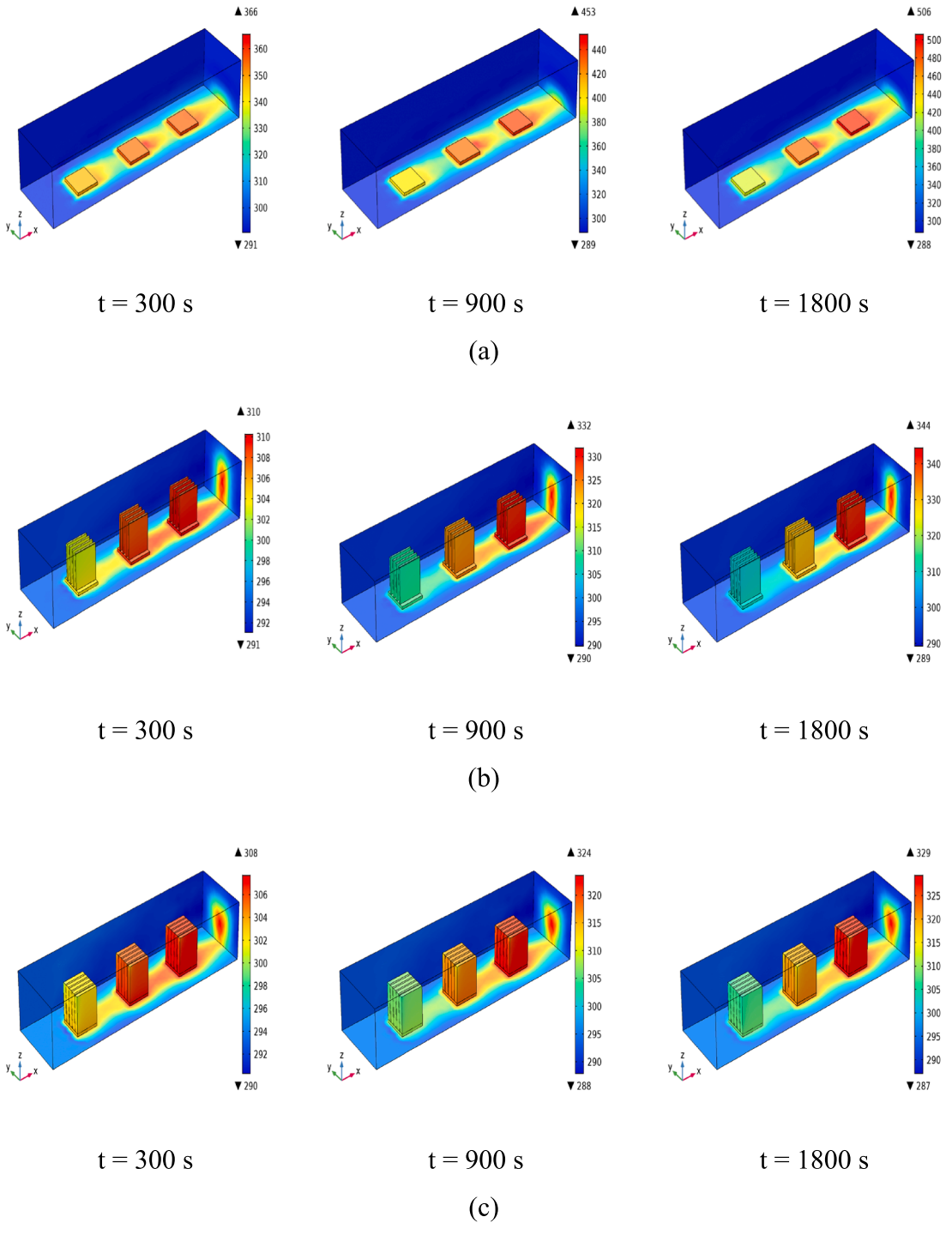

Fig. 5. Comparison of temperature distributions for (a) a clear channel and a channel with (b) FAHS and (c) FAFHSs; $q_w = 4$ W and inlet air velocity $U_{in} = 0.21$ m/s.

4. CFD details and validation

The governing equations of the above physical model are solved by COMSOL Multiphysics using the numerical finite element approach, and the computational domain consisted of meshes with triangular non-uniform distributed grid size meshes [26]. The Table 2 presented the grid independence study which compared three different mesh types with different sizes (normal, fine, and finer), with a total number of elements of approximately 263958, 688071, and 1914469, respectively. The maximum variations in pressure, air velocity, and temperature between the meshes were approximately $7e^{-5}$%, 0.25%, and 0.1%, respectively. A comparison of the simulation results using the three meshes shows that the fine mesh can be considered adequate for predicting the numerical results for the channel and FAFHSs.

Fig. 3 shows the variation of pressure and velocity versus the number of grid elements. The variation in pressure and velocity corresponding to a change in the number of grid elements is about 0.25% at most. In view of the computational time of the CFD analysis, the fine mesh type with 688,071 grid elements was used for the remainder computations for convenience.

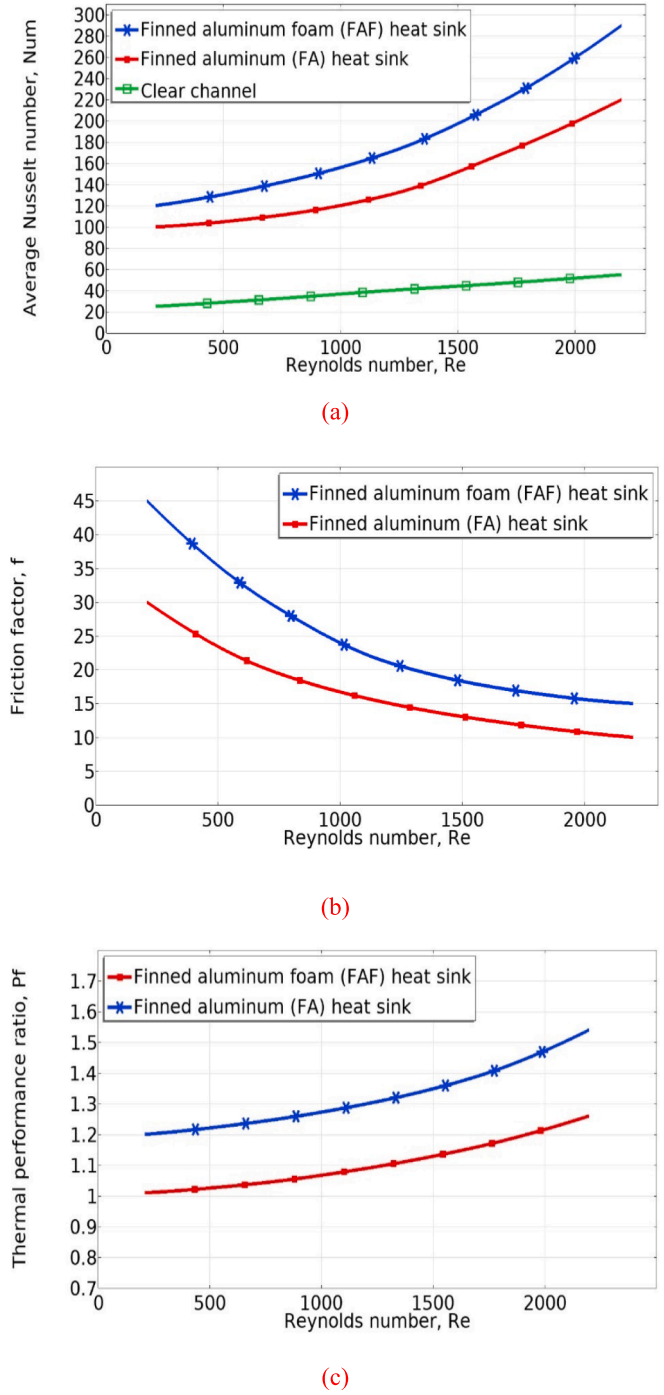

Fig. 6. Comparison of the (a) Nusselt number, (b) friction factor, and (c) thermal performance ratio versus Reynolds number for the first FAHS and FAFHS.

Lee and Vafai [27], Dukhan [24] and others have confirmed that solid and fluid phases of an air-cooled aluminum foam have approximately the same temperature. Therefore, in the present numerical simulation results, only the local equilibrium temperature is presented for the indicated temperature within the metal foam.

Fig. 4.a shows plots of validation of the CFD simulation results versus the experimental data within the 20 PPI aluminum foam, with $\varepsilon = 68.6\%$ and $U_{in} = 2.71$ m/s. The experimental data presented in the study of Dukhan et al. [24] are derived from thermal measurements of aluminum foams subjected to a constant heat flux. The non-dimensional temperature curves of the present CFD simulation and the experimental ones are presented versus the non-dimensional height distance, which corresponds to various positions of non-dimensional axial distance. The relationship of the temperature inside the aluminum foam to the distance follows an exponential curve, in which the temperature increases as the distance to the heated wall decreases.

Fig. 4.b shows comparisons of pressure drop versus inlet velocity with experimental results for FAHS and FAFHS. This comparison is made between the present CFD simulation results and the experimental data presented in a study by Feng et al [23]. The results predicted by the present simulation study are in good agreement with the published experimental results cited above, with a maximum deviation of 7.14% for the pressure drop. The discrepancies are mostly due to the experimental uncertainties and the values of the thermo-physical properties of the air used in the physical model and those used but not presented in reference [23].

Fig. 4.c shows a comparison between the numerical simulation results of the present study and those of the works of Bhattachariya [28] and DeGroot [29] with respect to the variation of the heat transfer coefficient with velocity. The results of this study are in perfect agreement with those of the above works, with a relative error of only 1.96%.

5. Results and discussion

5.1. Thermal-hydraulic performance comparisons

The transient three-dimensional temperature distributions for the finned aluminum foam heat sinks (FAFHSs), finned aluminum heat sinks (FAHSs), and clear channel are shown in Fig. 5. To better understand the temperature evolution during the cooling process inside the channel, three times were selected to present the simulation results: (t = 300 s) for the beginning of the cooling process, (t = 900 s) corresponding to the full evolution of the heating process by the thermal sources, and (t = 1800 s) for the establishment of forced convection cooling mode. As can be seen in Fig. 5.a, and for all the times cited above, inside the clear channel, the heat sources temperatures are relatively high, with maximum values equal to T = 366 K, T = 453 K and T = 506 K, respectively, corresponding to the specified times cited above, while the air temperature is relatively low, except for the regions behind the heat sources in the flow direction.

Fig. 5.b presents the simulation results of the temperature evolution inside the channel with multiple FAHSs. It is clearly seen that, in comparison with the case of the clear channel, the use of FAHSs significantly reduces the temperature distribution of the heat sources for the times mentioned above, with values of T = 310 K, T = 332 K and T = 344 K, respectively, but the temperature distribution of the aluminum fins and the heat sources remains high, and the air temperature is relatively low.

As shown in Fig. 5.c, and compared with the two previous cases of the clear channel and FAHSs, the use of the FAFHSs enables the reduction of the temperature distribution of the thermal sources and fins with T = 308 K, T = 324 K and T = 329 K, respectively, at the specified times cited above, while the internal air temperature is higher. This clearly indicates that the thermal characteristics and fluid flow performance of the FAFHSs are significantly improved, which favors their use in high-power electronics thermal management applications.

Fig. 6.a shows the variation of the corresponding average Nusselt numbers (Nu_m) with the Reynolds number (Re) for the clear channel, the FAHSs and FAFHSs. As expected, Nu_m increases with an increase in Re, and the variation becomes significant at higher Reynolds numbers for the last two cases cited above. At Re = 2000, Nu_m of the first FAFHS in the channel was 30% larger than that of the first FAHS. The FAFHS has a better Nu_m compared with the clear channel and FAHSs cases because of the enhanced effective thermal conductivity, which is related to the addition of aluminum fins to the fins of aluminum foam. Consequently, more heat flux is transferred by conduction from the thermal sources via the aluminum fins and then dissipated by forced convection to the cooling fluid.

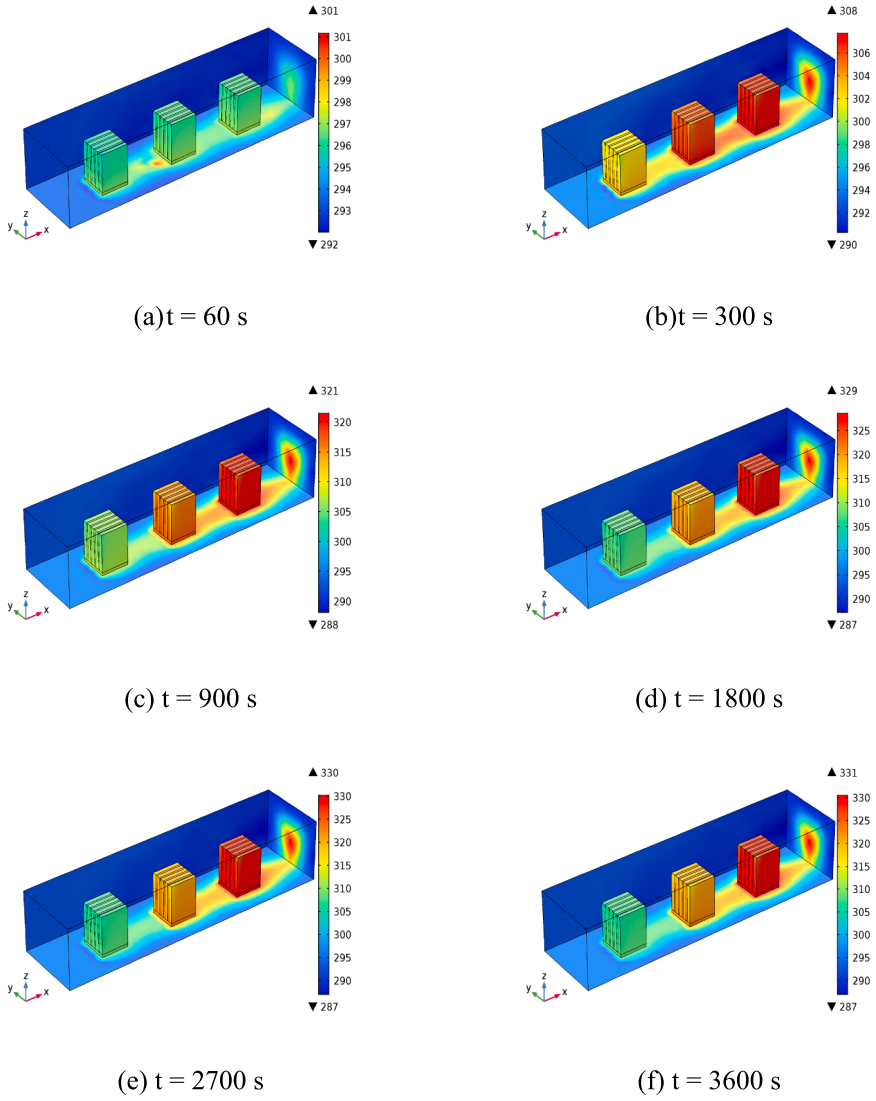

Fig. 7. Transient thermal behavior of FAFHSs at U_{in} = 0.21 m/s.

Fig. 6.b shows the variation of the friction factor as a function of Reynolds number for the first FAFHS and FAHS heat sinks. The friction factors of both configurations decrease with increasing Reynolds number; however, the friction factor of FAFHS is larger than that of FAHS. Aluminum foam, with its porous structure, offers more contact area with air, which increases resistance to air flow and causes a significant pressure drop.

The thermal performance ratio (P_f) of the FAFHS was calculated by considering the thermal enhancement and pressure drop, as given by Equation (16), Fig. 6.c shows a comparison of the thermal performance of the first FAHS and FAFHS versus Re. As can be seen in the figure, P_f for the two types of heat sinks increases as Re increases. At Re = 2000, the P_f of the FAFHS is 23.14% larger than the FAHS. Consequently, the FAFHS is the most appropriate electronic cooling management configuration.

5.2. Thermal-hydraulic behavior

In the present transient CFD simulation, each FAFHS in the horizontal channel is heated from below using a constant flux heat source, q_w = 4 W. To mimic the temperature rise in electronic equipment and to understand the FAF heat sink cooling process in a forced convection environment, the FAFHS were heated from room temperature (near 24.5 °C), where the air velocity at the inlet of the channel has a constant value. Our main concern in this study is to determine the cooling performance under a constant flux heat source, while varying the inlet air velocity, and with variable morphological properties of the aluminum foam: porosity (ε) varying from 0.85 to 0.95.

Under the fixed parameters of thermal source heat flux q_w = 4 W, inlet air velocity U_{in} = 0.21 m/s, porosity ε = 0.95, and density of porosity PPI = 30, Fig. 7 shows the temperature distribution within the channel for various times, i.e., t = 60, 300, 900, 1800, 2700, and 3600 s. initially, and at the time t = 60 s, the temperatures of the thermal sources are close to the ambient temperature T_{am}. Subsequently, at t = 300 s, the FAFHS are fully heated, and the temperature increases further to reach T = 302 K for the first FAHS, and T = 306 K for the second and third FAFHS. At t = 900 s, the FAHS heat up further to reach T = 305 K, T = 315 K, and T = 320 K for the first, second and third FAFHS, respectively. From the moment t = 1800 s, the temperatures of the FAFHS are almost constant, and the progress of the forced cooling process proceeds until time t = 3600 s, demonstrating that the first heat sink is cooled at an average temperature close to T = 308 K, the second at T = 320 K, and the third at T = 330 K.

The heat generated by the thermal sources to the FAFHSs was used to imitate the temperature increase in electronic devices. Fig. 8 shows the average temperature evolution of FAFHS's base, aluminum fin, and aluminum foam fin for each FAFHS in the channel versus time. Under

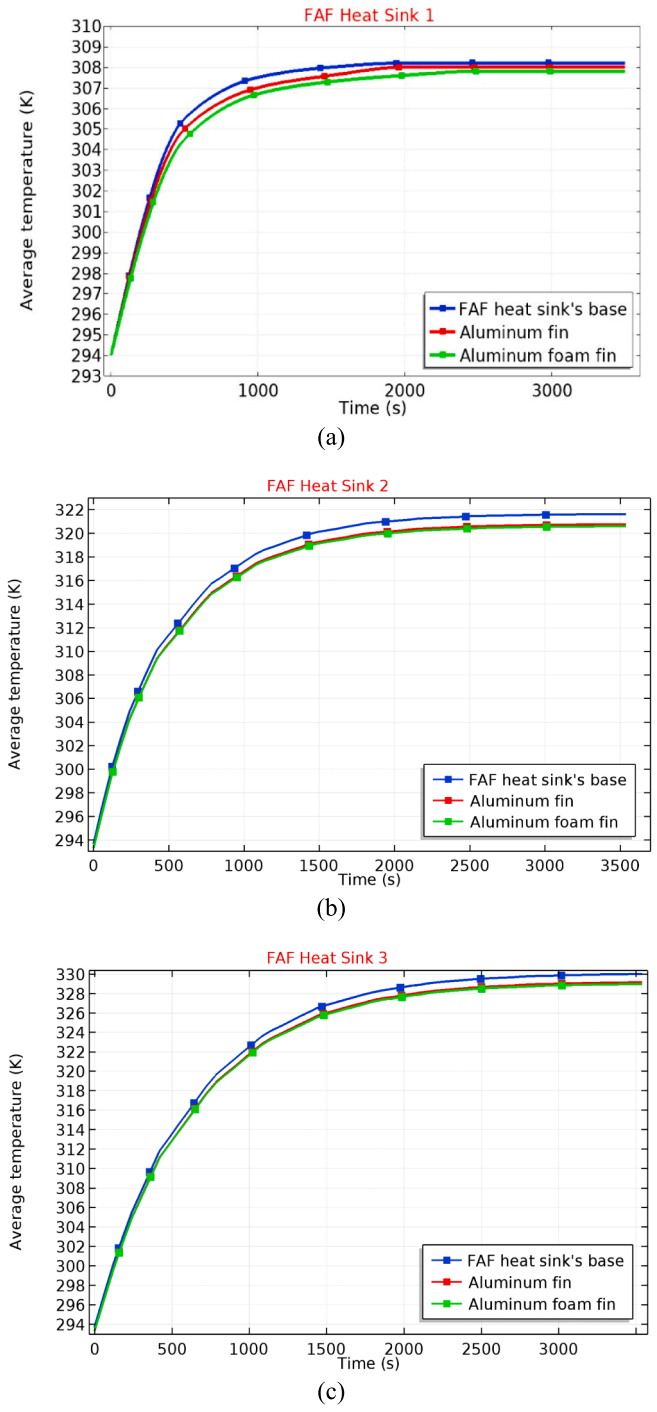

Fig. 8. Transient temperatures of the FAFHSs and thermal sources.

the following fixed parameters, i.e., thermal source power $q_w = 4$ W, inlet air velocity $U_{in} = 0.21$ m/s, porosity $\varepsilon = 0.95$, and density of porosity PPI = 30, the heating process is performed by conjugate heat transfer, by heat conduction from the aluminum fins, and by conduction and convection heat from the fins made of aluminum foam. As can be seen in the Fig. 8.a, for the first FAFHS, the temperatures of FAFHS's base, aluminum fin, and aluminum foam fin increase with time until the thermal study state is reached, when these temperatures reach 308.2 K, 308 K, and 307.8 K, respectively. Fig. 8.b and 8.c show the same behavior for the second and third FAFHSs, showing higher temperatures than the first FAFHS.

The 3D transient velocity profile of the cooling fluid inside the channel is shown in Fig. 9.a. To cover the entire cooling time of the thermal sources in forced convection, we chose three different times to represent the evolution of fluid velocity and pressure within the channel: t = 60 s, t = 1800 s, and t = 3600 s. As shown in the Fig. 9.a, the air flows through the aluminum foam fins (porous medium) of the FAFHSs with a low velocity V = 0.05 m/s, this is due to the velocity at the pore given by $V_p = U_{in}/d_p$ [22], where d_p is the pore diameter of the aluminum foam. However, to maintain the continuity of the air flow within the channel, the velocity in front and at the lateral sides of the FAFHSs takes relatively high value V = 0.5 m/s. As can be seen, and as a result of the low inlet velocity of the air $U_{in} = 0.21$ m/s, the transient velocity profile for the three times mentioned above is almost similar.

Fig. 9.b shows the pressure evolution of the cooling fluid within the channel as a function of time, which is represented by three values: t = 60 s, t = 1800 s, and t = 3600 s. As mentioned above for the case of the evolution of the air velocity within the channel as function of time, and as a result of the low inlet velocity of air, the evolution of the pressure within the channel is almost identical for the times mentioned above. The air pressure takes relatively high values at the first FAFHS, relatively medium at the second, and low at the third.

5.3. *Porosity effect*

In this section, the effect of aluminum foam porosity on the thermal–hydraulic characteristics and performance of the first air-cooled FAFHS is presented. Table 3 presents the properties of the aluminum alloy T-6201 with various porosities.

The Nu_m of the first FAFHS in the channel with various porosities increases with Re. As can be seen in Fig. 10.a, Nu_m decreases as the metal foam porosity increases. Under the conditions of heat input of $q_w = 4$ W and PPI metal foam of 30, the 85% porosity shows a relatively higher Nu_m compared with the other aluminum foams because of the greater number of fiber ligaments and the greater surface area for heat transfer. If the porosity of the aluminum foam increases, this leads to an increase in pore size, which reduces the total surface area available for heat exchange with the fluid. Thus, thermal convection decreases and the Nusselt number also decreases. In addition, increased porosity can lead to increased pressure drop, which reduces the thermal efficiency of the metal foam heat sink. Consequently, low porosity is preferred to maximize the thermal performance of the metal foam heat sink.

Fig. 10.b shows the variation of the average pressure drop inside the first FAFHS in the channel with Re for various aluminum foam porosities. As the porosity increases, the average pressure drop increases. At Re = 2000, and for the porosities $\varepsilon = 0.95$, 0.925, 0.9 and 0.85 cited in the Table 3, the average pressure drop takes the following values 3.15, 2.9, 2.6 and 2.5 Pa/m, respectively, which shows the growth of the average pressure drop with increasing porosity. The pressure drop in aluminum foam is primarily due to viscous friction between the fluid and the foam walls. An increase in porosity means that there are more voids and less solid material to guide the fluid flow, which increases the viscous friction. In other words, although the increase in porosity may increase the heat transfer surface area, it is more than offset by the increase in viscous friction, resulting in an increase in pressure drop in the metal foam. Thus, the decrease in flow resistance is offset by the increase in viscous friction.

Fig. 10.c shows the variation of the thermal performance ratio P_f for the first FAFHS in the channel with Re with various porosities. The thermal-performance ratio decreases as the porosity of the aluminum foam increases. It can be easily seen in this figure that with a porosity of 85%, FAFHS has the best thermal performance ratio compared to other porosity values due to the larger heat exchange area.

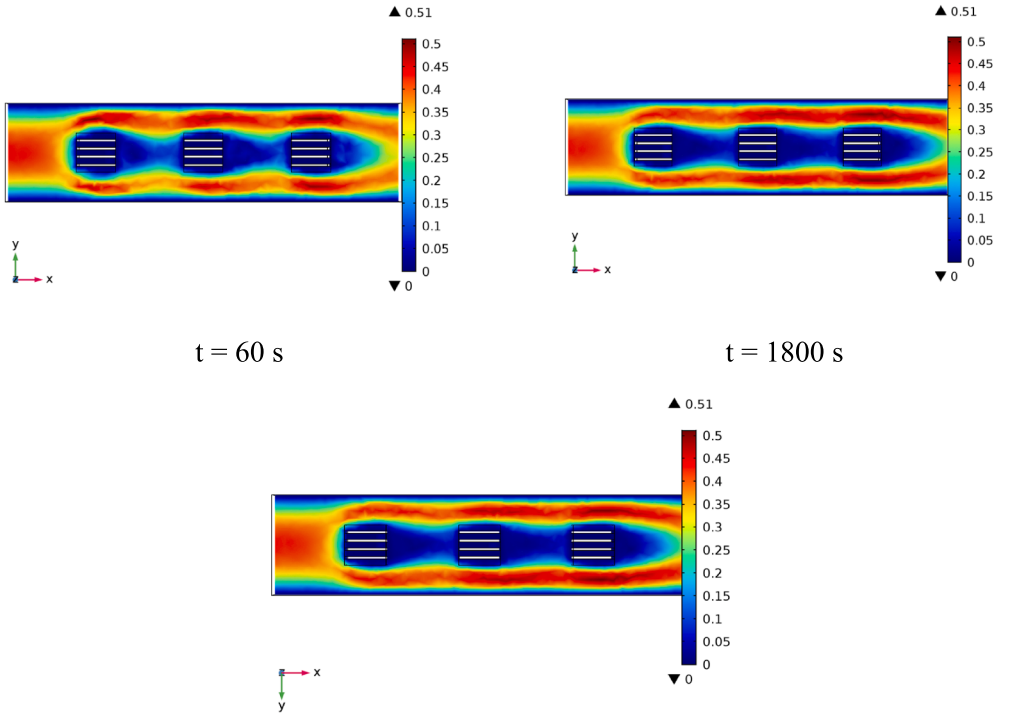

t = 60 s t = 1800 s

t = 3600 s.

(a)

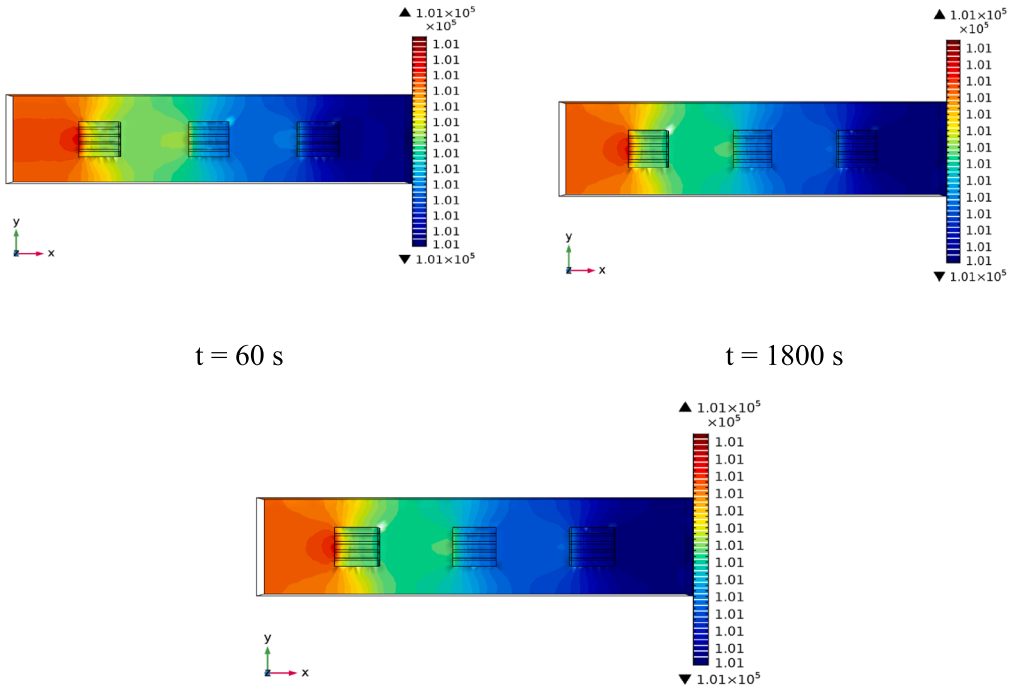

t = 60 s t = 1800 s

t = 3600 s

(b)

Fig. 9. Transient (a) air velocity and (b) pressure inside the channel.

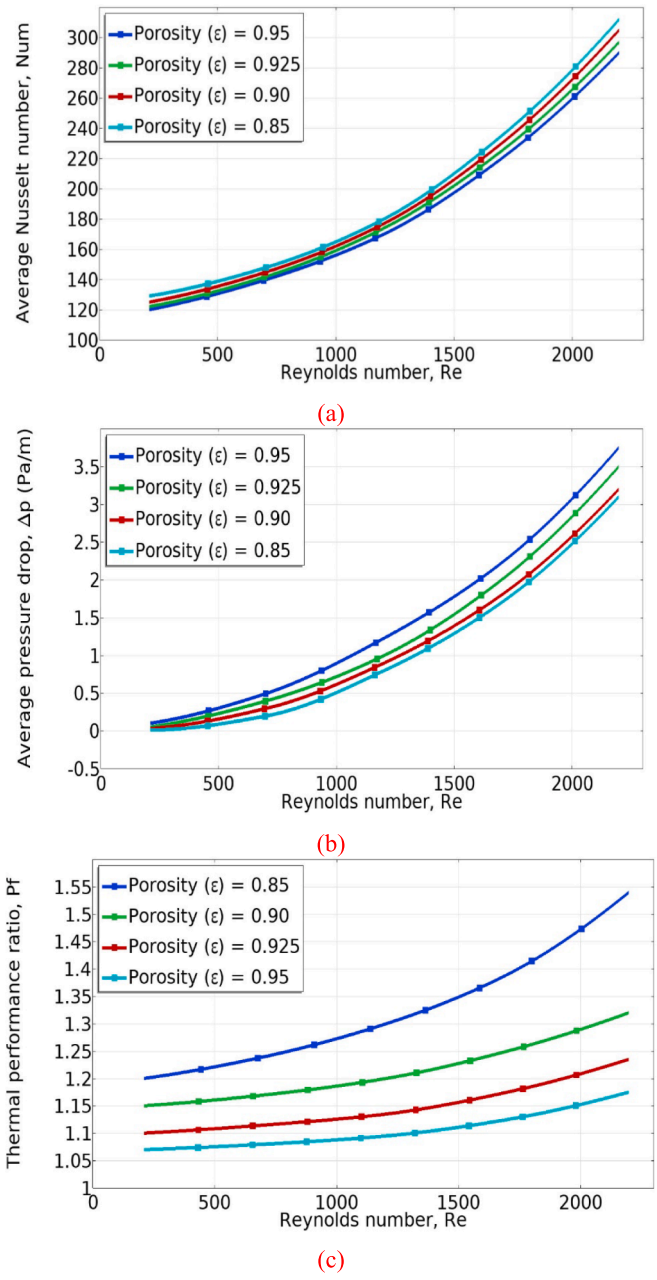

Fig. 10. Porosity effect on the thermal fluid characteristics for the first air-cooled FAFHS with heat input of 4 W: (a) average Nusselt number, (b) average pressure drop, and (c) thermal performance ratio.

6. Conclusions

In this study, three-dimensional transient numerical simulations of forced convective flow of air in a horizontal channel equipped with FAFHSs were carried out using commercial COMSOL. An array of FAFHSs was mounted on thermal sources and placed on the lower plate inside a horizontal channel. The transient thermal-hydraulic behavior and performance of the FAFHSs were studied and analyzed under conditions of a constant flux heat source, while varying the inlet air velocity, and aluminum foam porosity.

The simulation results were compared with the experimental results and showed good agreement. The main conclusions of this study are as follows:

- Under the combined effects of the aluminum fins and aluminum foam fins on the enhancement of the thermal characteristics and performance, Nu_m and P_f of the FAFHS are 30% and 23.14% respectively larger than that of the AFHS at Re = 2000.
- Average temperatures of FAFHS's base, aluminum fin, and aluminum foam fin of the FAFHS increase with time until the thermal study state is reached, when the second and third FAF heat sinks, showing higher temperatures than the first FAFHS.
- As a result of a low inlet velocity of air, the transient velocity profile for three different times mentioned above is almost similar. The air flows through the aluminum foam fins (porous medium) of the FAFHS with a low velocity, however in front and at the lateral sides of the FAFHS the air velocity takes relatively high value.
- The evolution of the air pressure in the channel is almost identical for all the times mentioned above. The pressure takes relatively high values at the first FAFHS, relatively medium at the second, and low at the third.
- As the aluminum foam porosity increased from 0.85 to 0.95, the Nu_m and P_f decreased, while the pressure drop increased. Consequently, to obtain better thermal–hydraulic characteristics and performance, the internal morphological parameters of the AF should be optimized.

Declaration of Competing Interest

The authors declare that they have no known competing financial interests or personal relationships that could have appeared to influence the work reported in this paper.

Acknowledgements

This research work was funded by Institutional Fund Projects under grant no (IFPIP-204-130-1443). The authors gratefully acknowledge technical and financial support provided by the ministry of Education and King Abdulaziz University, DSR, Jeddah, Saudi Arabia.

References

[1] G. Bamorovat Abadi, K.C. Kim, Experimental heat transfer and pressure drop in a metal-foam-filled tube heat exchanger, Exp. Therm Fluid Sci. 82 (2017) 42–49, https://doi.org/10.1016/j.expthermflusci.2016.10.031.
[2] N. Dukhan, Metal foams: fundamentals and applications, DEStech Publications, Inc, 2013.
[3] S.G. Kandlikar, Review and projections of integrated cooling systems for three-dimensional integrated circuits, J. Electron. Packag. 136 (2014), https://doi.org/10.1115/1.4027175.
[4] K. Nawaz, J. Bock, A.M. Jacobi, Thermal-hydraulic performance of metal foam heat exchangers under dry operating conditions, Appl. Therm. Eng. 119 (2017) 222–232, https://doi.org/10.1016/j.applthermaleng.2017.03.056.
[5] S.P. Aly, Thermo-Mechanical Behavior of Metal Foams - A Computational and Experimental Approach, 2015. https://doi.org/10.13140/RG.2.2.18206.79689.
[6] M.P. Orihuela, F. Shikh Anuar, I. Ashtiani Abdi, M. Odabaee, K. Hooman, Thermohydraulics of a metal foam-filled annulus, Int. J. Heat Mass Transf. 117 (2018) 95–106, https://doi.org/10.1016/j.ijheatmasstransfer.2017.10.009.
[7] H.J. Xu, Z.B. Xing, F.Q. Wang, Z.M. Cheng, Review on heat conduction, heat convection, thermal radiation and phase change heat transfer of nanofluids in porous media: fundamentals and applications, Chem. Eng. Sci. 195 (2019) 462–483, https://doi.org/10.1016/j.ces.2018.09.045.
[8] S. Rashidi, M.H. Kashefi, K.C. Kim, O. Samimi-Abianeh, Potentials of porous materials for energy management in heat exchangers – a comprehensive review, Appl. Energy 243 (2019) 206–232, https://doi.org/10.1016/j.apenergy.2019.03.200.
[9] J.R. Bose, S. Manova, L.G. Asirvatham, S. Wongwises, Comprehensive case study on heat transfer enhancement using micro pore metal foams: from solar collectors to thermo electric generator applications, Case Stud. Therm. Eng. 27 (2021), 101333, https://doi.org/10.1016/j.csite.2021.101333.
[10] H. Peng, M. Li, F. Hu, S. Feng, Performance analysis of absorber tube in parabolic trough solar collector inserted with semi-annular and fin shape metal foam hybrid structure, Case Stud. Thermal Eng. 26 (2021), 101112, https://doi.org/10.1016/j.csite.2021.101112.
[11] M. Sharaf, A.S. Huzayyin, M.S. Yousef, Performance enhancement of photovoltaic cells using phase change material (PCM) in winter, Alex. Eng. J. 61 (2022) 4229–4239, https://doi.org/10.1016/j.aej.2021.09.044.

[12] S.A.M. Mehryan, M.H. Heidarshenas, A. Hajjar, M. Ghalambaz, Numerical study of melting-process of a non-Newtonian fluid inside a metal foam, Alex. Eng. J. 59 (2020) 191–207, https://doi.org/10.1016/j.aej.2019.12.021.
[13] L. Gang, X. Tian, W. Xinyi, Y. Xiaohu, L. Hailong, Numerical analysis of inner heating tube position for improving solid-phase transition in a shell-and-tube heat accumulator, Alex. Eng. J. 65 (2023) 771–784, https://doi.org/10.1016/j.aej.2022.10.022.
[14] N. Dukhan, Ö. Bağcı, M. Özdemir, Metal foam hydrodynamics: Flow regimes from pre-Darcy to turbulent, Int. J. Heat Mass Transf. 77 (2014) 114–123, https://doi.org/10.1016/j.ijheatmasstransfer.2014.05.017.
[15] A.S. Suleiman, N. Dukhan, Forced convection inside metal foam: Simulation over a long domain and analytical validation, Int. J. Therm. Sci. 86 (2014) 104–114, https://doi.org/10.1016/j.ijthermalsci.2014.06.022.
[16] N. Dukhan, M. Özdemir, L. Kavurmacıoğlu, Experimental fully-developed thermal convection for non-darcy water flow in metal foam, J. Therm. Eng. 2 (2016) 677–682. https://doi.org/10.18186/jte.46830.
[17] A.M. Bayomy, M.Z. Saghir, T. Yousefi, Electronic cooling using water flow in aluminum metal foam heat sink: experimental and numerical approach, Int. J. Therm. Sci. 109 (2016) 182–200, https://doi.org/10.1016/j.ijthermalsci.2016.06.007.
[18] M. Paknezhad, A.M. Rashidi, T. Yousefi, Z. Saghir, Effect of aluminum-foam heat sink on inclined hot surface temperature in the case of free convection heat transfer, Case Stud. Therm. Eng. 10 (2017) 199–206, https://doi.org/10.1016/j.csite.2017.06.007.
[19] S.K. Mohammadian, Y. Zhang, Cumulative effects of using pin fin heat sink and porous metal foam on thermal management of lithium-ion batteries, Appl. Therm. Eng. 118 (2017) 375–384, https://doi.org/10.1016/j.applthermaleng.2017.02.121.
[20] Y. Li, L. Gong, M. Xu, Y. Joshi, Enhancing the performance of aluminum foam heat sinks through integrated pin fins, Int. J. Heat Mass Transf. 151 (2020), 119376, https://doi.org/10.1016/j.ijheatmasstransfer.2020.119376.
[21] N. Donald A, B. Adrian, Convection in Porous Media, Springer New York, 2006. https://doi.org/10.1007/0-387-33431-9.
[22] B. Kotresha, N. Gnanasekaran, C. Balaji, Numerical simulations of flow-assisted mixed convection in a vertical channel filled with high porosity metal foams, Heat Transfer Eng. 41 (2020) 739–750, https://doi.org/10.1080/01457632.2018.1564208.
[23] S.S. Feng, J.J. Kuang, T. Wen, T.J. Lu, K. Ichimiya, An experimental and numerical study of finned metal foam heat sinks under impinging air jet cooling, Int. J. Heat Mass Transf. 77 (2014) 1063–1074, https://doi.org/10.1016/j.ijheatmasstransfer.2014.05.053.
[24] N. Dukhan, K.-C. Chen, Heat transfer measurements in metal foam subjected to constant heat flux, Exp. Therm Fluid Sci. 32 (2007) 624–631, https://doi.org/10.1016/j.expthermflusci.2007.08.004.
[25] Y. Li, L. Gong, M. Xu, Y. Joshi, Hydraulic and thermal performances of metal foam and pin fin hybrid heat sink, Appl. Therm. Eng. 166 (2020), 114665, https://doi.org/10.1016/j.applthermaleng.2019.114665.
[26] Y.W. Kwon, F. Kreith, H. Bang, The Finite Element Method Using MATLAB, 2nd ed., CRC Press, Boca Raton, 2017. https://doi.org/10.1201/9781315275949.
[27] D.-Y. Lee, K. Vafai, Analytical characterization and conceptual assessment of solid and fluid temperature differentials in porous media, Int. J. Heat Mass Transf. 42 (1999) 423–435, https://doi.org/10.1016/S0017-9310(98)00185-9.
[28] A. Bhattacharya, R.L. Mahajan, Finned metal foam heat sinks for electronics cooling in forced convection, J. Electron. Packag. 124 (2002) 155–163, https://doi.org/10.1115/1.1464877.
[29] C.T. DeGroot, A.G. Straatman, L.J. Betchen, Modeling forced convection in finned metal foam heat sinks, J. Electron. Packag. 131 (2009), https://doi.org/10.1115/1.3103934.
[30] C.-C. Chen, P.-C. Huang, H.-Y. Hwang, Enhanced forced convective cooling of heat sources by metal-foam porous layers, Int. J. Heat Mass Transf. 58 (2013) 356–373, https://doi.org/10.1016/j.ijheatmasstransfer.2012.11.041.